Mon. Not. R. Astron. Soc. **000**, 1–5 (XXX) Printed 7 November 2014 (MN LATEX style file v2.2)

A new isolated dSph galaxy near the Local Group

I. D. Karachentsev[1⋆], L. N. Makarova[1], D. I. Makarov[1], R. B. Tully[2], L. Rizzi[3]
[1] *Special Astrophysical Observatory, Nizhniy Arkhyz, Karachai-Cherkessia 369167, Russia*
[2] *Institute for Astronomy, University of Hawaii, 2680 Woodlawn Drive, HI 96822, USA*
[3] *W. M. Keck Observatory, 65-1120 Mamalahoa Hwy, Kamuela, HI 96743, USA*

arXiv:1411.1674v1 [astro-ph.GA] 6 Nov 2014

Accepted XXX. Received XXX; in original form XXX

ABSTRACT
Observations of the highly isolated dwarf spheroidal galaxy KKs 3 = [KK2000] 03 with the Hubble Space Telescope (HST) Advanced Camera for Surveys (ACS) are presented. We measured the galaxy distance of 2.12 ± 0.07 Mpc using the Tip of Red Giant Branch (TRGB) method. The total blue absolute magnitude of the galaxy is estimated as $M_B = -10.8$ mag. We briefly discuss the star formation history of KKs 3 derived from its colour-magnitude diagram. According to our calculation, the total stellar mass of the galaxy is $2.3 \times 10^7 M_\odot$, and most stars (74%) were formed at an early epoch more than 12 Gyr ago. A full description of the properties of the colour-magnitude diagram requires some extension of star formation in metallicity and age.

Key words: galaxies: dwarf – galaxies: distances and redshifts – galaxies: stellar content – galaxies:individual: KKs 3

1 INTRODUCTION

In the standard cosmological model, ΛCDM, the formation of galaxies begins with the hierarchical merging of dwarf objects (White & Rees 1978). The dwarf galaxies that survive until today are sensitive to their environment, given their shallow potential wells and characteristic internal motions of 5 to 30 km s^{-1}. Gas-rich dwarf irregular (dIrr) galaxies with active star formation are common in the general field and the outer regions of groups. The gas-poor dwarf spheroidal systems (dSph) with old stellar population are found almost exclusively in the virial domain of groups and clusters. It is generally considered that the concentration of dSph galaxies to the halos of massive galaxies is due to processes of gas stripping and strangulation of irregular dwarfs that limits further star formation, transforming dIrr into dSph. If these mechanisms that are operative in dense environments are paramount then dSph objects should be absent in the general field of low densities. However, energetic events associated with active star formation in dwarf systems at an early epoch might deplete gas resources. In such cases, relic quenched dSph galaxies may occur among isolated objects. Alternatively, Benítez-Llambay et al. (2013) offer an intermediate mechanism, with the transformation of dIrr galaxies into dSphs occurring any time via so-called "cosmic web stripping".

Beyond the issue of the relationship between dIrr and dSph, the search and discovery of isolated spheroidal dwarfs constitutes an important interest for cosmology, given the unexpectedly small number of dwarfs of any type. Over the last decade, about 30 dSph galaxies have been discovered in the Local Group through systematic search in the vicinity of M 31 (Martin et al. 2013) and more that a dozen dSphs were discovered by Chiboucas et al. (2009) in the nearby group around M 81. The discoveries resulted from targeted searches within small parts of the sky (~ 390 deg^2 and ~ 65 deg^2, respectively). The hunt for isolated spheroidal dwarfs is very difficult because it requires a survey of large sky area and considerable sensitivity. Objects devoid of neutral hydrogen and high contrast H II-regions are usually invisible in optical and H I-surveys. Only very nearby dSph galaxies, inevitably of low surface brightness, may be revealed if they resolve into individual stars.

Since 2008, only three galaxies had been newly discovered in a spherical shell between radii 1 and 3 Mpc around the Local Group. Two of them are dIrrs, UGC 4879 (Kopylov et al. 2008) and Leo P (Giovanelli et al. 2013), and the third one, KK 258 (Karachentsev et al. 2014), belongs to the transition type dTr with minimal but detectable gas and young stars. Here we report the discovery in this volume of a dwarf spheroidal system KKs 3 ([KK2000] 03 = SGC 0224.3–7345 in the nomenclature of the NASA/IPAC Extragalactic Database) at a distance of $D = 2.12 \pm 0.07$ Mpc and well removed from any other known galaxy.

⋆ E-mail: ikar@sao.ru

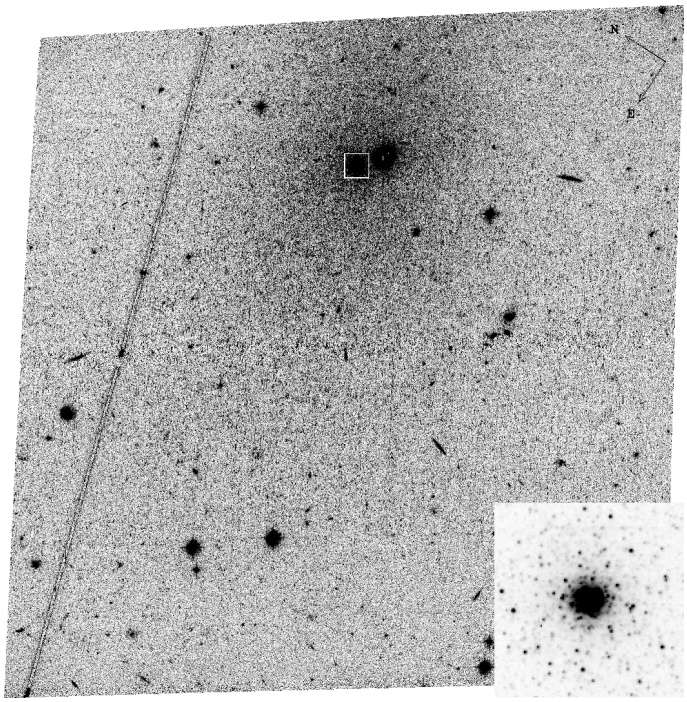

Figure 1. *HST*/ACS image of KKs 3 through the *F606W* filter. The image size is 3.4 × 3.4 arcmin. The 7.5 arcsec region highlighted by the white square near the centre of the galaxy is shown in the lower right corner to contain a globular cluster.

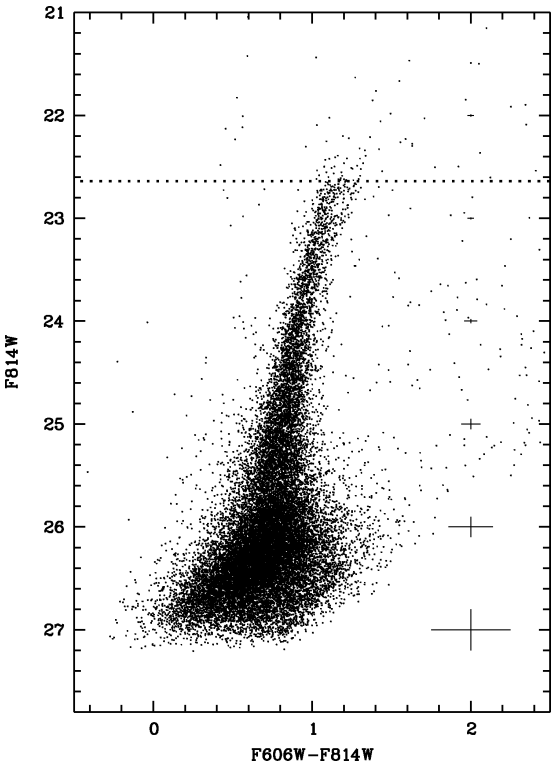

Figure 2. Colour-magnitude diagram of KKs 3. Photometric errors are indicated by the bars at the right side of the CMD. The TRGB position is indicated by the dotted line.

2 ACS HST OBSERVATIONS AND TRGB DISTANCE

The low surface brightness object KKs 3 with J2000 coordinates: R.A. = $02^h24^m44\overset{s}{.}4$, Dec. = $-73°30'51''$ was detected in full sky surveys by Karachentseva & Karachentsev (2000) and Whiting et al. (2002) as a potential dSph galaxy neighbouring the Local Group. Even earlier, the object was recorded by Corwin et al. (1985). In HyperLeda[1] the galaxy is listed as PGC 09140. The 'Updated Nearby Galaxy Catalog' (Karachentsev et al. 2013) assigns KKs 3 the total apparent magnitude $B = 16.0$ mag and the Holmberg diameters 2.5×1.0 arcmin. The assigned distance of 4 Mpc in that catalogue erroneously assumed an association of KKs 3 with the galaxy NGC 1313. Kirby et al. (2008) imaged KKs 3 at the 3.9-m AAT telescope in H-band and noted it as almost invisible with an 1800 s exposure.

The dwarf galaxy KKs 3 was observed aboard *HST* using Advanced Camera for Surveys (ACS) on 29 August, 2014 (SNAP 13442, PI R. Tully). Two exposures were made in a single orbit with the filters *F606W* (1200 s) and *F814W* (1200 s). The *F606W* image of the galaxy KKs 3 is shown in Fig. 1. In the central part of the galaxy, highlighted by the white square, we found a globular cluster shown in the lower right corner of the Fig. 1. Photometry of the cluster yields its total magnitude $V = 18.30 \pm 0.03$ mag and the colour $V - I = 0.89 \pm 0.06$. The bright spot at the center of the galaxy, just to the right of the globular cluster box is caused by a tight pair of red foreground stars.

The photometry of resolved stars in the galaxy was performed with the ACS module of the DOLPHOT package[2] for crowded field photometry (Dolphin 2002) using the recommended recipe and parameters. Only stars with photometry of good quality were included in the final compilation, following recommendations given in the DOLPHOT User's Guide.

Artificial stars were inserted and recovered using the same reduction procedures to accurately estimate photometric errors, including crowding and blending effects. A large library of artificial stars was generated spanning the full range of observed stellar magnitudes and colours to assure that the distribution of the recovered photometry is adequately sampled.

We have determined the KKs 3 distance with our TRGBTOOL program which uses a maximum-likelihood algorithm to determine the magnitude of the tip of the red giant branch (TRGB) from the stellar luminosity function (Makarov et al. 2006). The estimated value of the TRGB is $F814W = 22.64 \pm 0.04$ mag in the ACS instrumental system. Following the calibration of the TRGB methodology developed by Rizzi et al. (2007), we have obtained the true distance modulus $(m - M)_0 = 26.63 \pm 0.07$ mag and the distance of $D = 2.12 \pm 0.07$ Mpc. This measurement assumes foreground reddening of E(B-V) = 0.045 (Schlafly & Finkbeiner 2011).

[1] http://leda.univ-lyon1.fr

[2] http://purcell.as.arizona.edu/dolphot/

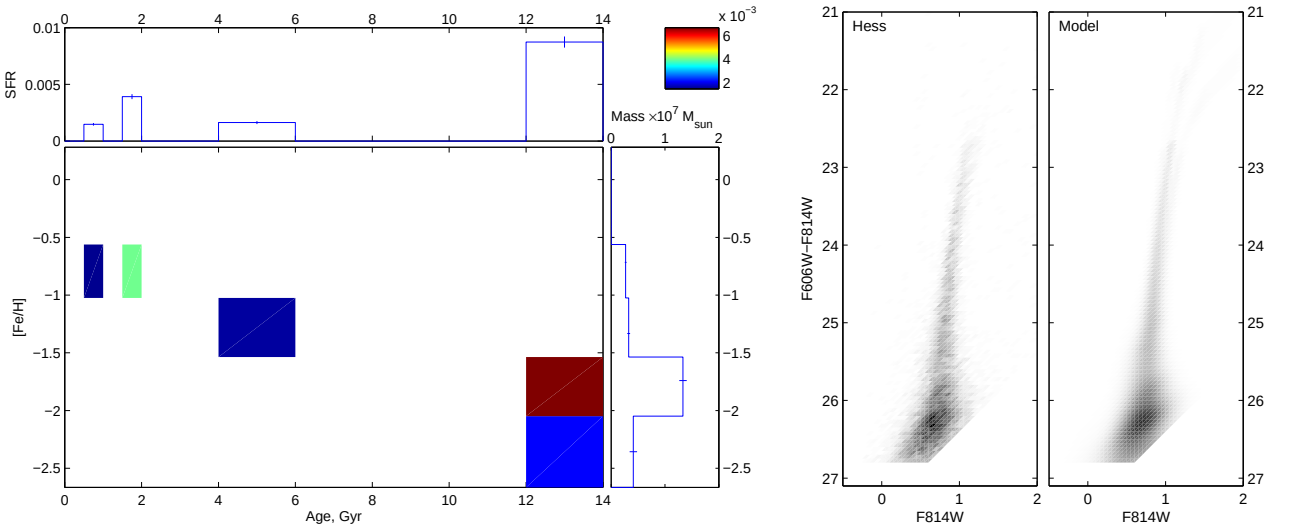

Figure 3. Left plot: The star formation history of KKs 3. The top panel shows the star formation rate (SFR) ($M_\odot\,\mathrm{yr}^{-1}$) against the age of the stellar populations. The bottom panel shows the metallicity of the stellar components as a function of age. The side panel plots stellar mass vs. metallicity. The resulting errors in the SFR are indicated with the vertical bars. These errors only represent the statistical uncertainties of the fit. Right plot: Observational (left) and reconstructed (right) colour-magnitude diagrams of KKs 3. The grey-scale density encodes the number of stars in a bin.

3 COLOUR-MAGNITUDE DIAGRAM AND STAR FORMATION HISTORY

Figure 2 shows the colour-magnitude diagram (CMD) of KKs 3. The measured TRGB position is marked by the dotted line. The variety of resolved stellar populations is not large in this picture. We can see a tight and well populated red giant branch (RGB) and a clearly visible red clump toward the bottom of the RGB in the magnitude range $25.8 \leqslant F814W \leqslant 26.8$. Asymptotic giant branch (AGB) stars in the one magnitude interval brighter than the TRGB are scarce. The few stars with the colour index of about 0.5–0.6 and $F814W$ between 21 and 24 mag are most likely foreground objects. They are randomly scattered on the ACS image rather than concentrate on the galaxy body. The lack of manifestations of star formation within the last Gyr puts an extreme limit on recent activity. According to the colour-magnitude diagram, the galaxy under study should be classified as a typical dwarf spheroidal. H I is undetected although the line-of-sight is confused by the Magellanic Stream.

We determine the quantitative star formation and metal enrichment history of KKs 3 from the CMD using our StarProbe program. The program develops an approximation to the observed distribution of stars in the CMD using a positive linear combination of synthetic diagrams formed by simple stellar populations (SSP: sets of single age and single metallicity populations). We used the Padova2000 theoretical isochrones (Girardi et al. 2000) and a Salpeter (1955) initial mass function (IMF). The synthetic diagrams were altered by the same incompleteness, crowding effects, and photometric systematics as those determined for the observations using artificial star experiments. A full description of the details of our approach and the StarProbe software are given in the papers of Makarov & Makarova (2004); Makarova et al. (2010). Figure 3 demonstrates the result of our calculations of the star formation history (SFH) of the KKs 3 dwarf galaxy. The uncertainty of each star formation episode is estimated from an analysis of the likelihood function. Upper and lower error bars are calculated for a significance level of 0.317, which corresponds to 1σ for a normal distribution. The errors only reflect statistical uncertainties of the fit. Systematic uncertainties caused by the isochrone set, the IMF choice, the distance and reddening estimates are not included in error bars.

Three star formation episodes are distinguished. The most prominent old star burst occurred 12–14 Gyr ago, the middle-age population was formed about 5 Gyr ago and there is evidence for the existence of even younger stars with age $\leqslant$ 2 Gyr. Note that the model anticipates more AGB stars than are seen in the observed CMD. The clearly visible red clump, helium burning stars at the base of the AGB, plays an important role in the age and metallicity reconstruction. The oldest population ($\sim$ 13 Gyr) gives a red clump that is too faint. The presence of a younger component populates a brighter red clump in accordance with the observations. However, the contribution of this younger population is small in stellar mass and star formation rate. A lower limit in age is established by the absence of main sequence or blue loop features.

According to our calculations, the total stellar mass of KKs 3 is $2.3{\times}10^7\,M_\odot$, and most of the stars were formed in the early epoch of the Universe 12–14 Gyr ago. We estimate the mass fraction formed during this initial event to be 74 per cent. The average rate of star formation in this period was high, $8.7 \pm 0.4 \times 10^{-3}\,M_\odot\,\mathrm{yr}^{-1}$. It can be seen from the Fig. 3, that the average metallicity of the primordial stars is extremely low, [Fe/H]$\simeq -1.9$. Less intensive star formation is noticeable about 4–6 and 0.8–2 Gyr ago. These episodes contribute about 14 per cent and 12 per cent of the total stellar mass, respectively. There is metal enrichment of the stars with time, with the youngest stars, at about 1 Gyr, most likely metal-enriched to [Fe/H]$\simeq -0.7$.

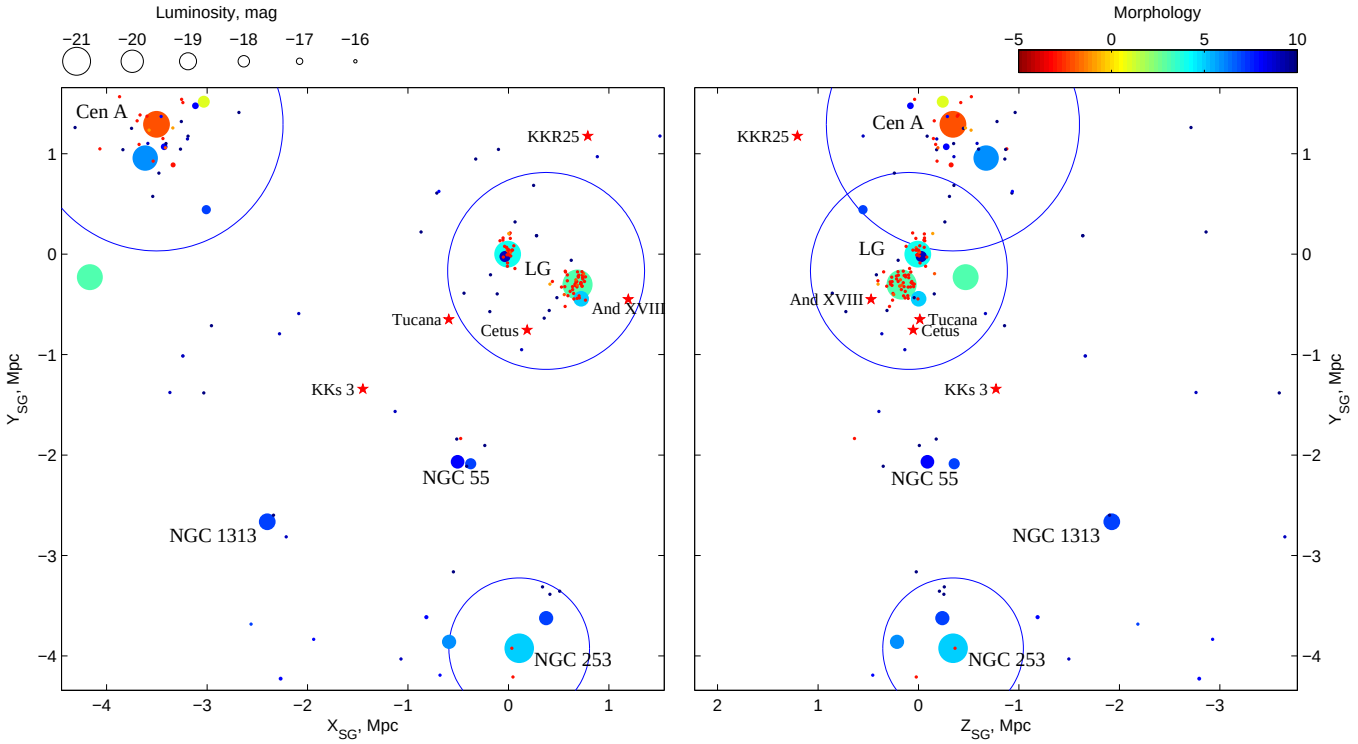

Figure 4. Landscape of neighbouring galaxies around KKs 3. The colour and size of the circles represent the morphological type and luminosity of a galaxy according to the given scales. Three circles outline spheres of zero-velocity surfaces around the three massive groups: the Local Group and groups around NGC 5128 (Cen A) and NGC 253. Red stars locate five dSph galaxies that in varying degrees are isolated systems.

4 ENVIRONMENT OF KKS 3 AND OTHER NEARBY DSPHS

The distribution of neighbouring galaxies in a cubic volume ±3 Mpc around KKs 3 is presented in the Fig. 4 in two Cartesian Supergalactic projections. The colour and size of the circles represent the morphological type and luminosity of the galaxies according to the given scales. In this volume there are three massive groups: the Local Group and groups around NGC 5128 (Cen A) and NGC 253. Three circles outline spheres of zero-velocity surfaces. Inside these domains group members do not participate in the cosmic expansion. At a little over 1 Mpc from KKs 3 there are also two small groups, one around NGC 55 and the other around NGC 1313. The nearest neighbours to our object are the following dwarf galaxies: IC 3104 ($M_B = -14.8$ mag, at 0.99 Mpc), ESO 294–010 ($M_B = -10.2$ mag, at 1.21 Mpc), IC 5152 ($M_B = -15.6$ mag, at 1.23 Mpc) and Tucana ($M_B = -9.2$ mag, at 1.34 Mpc). Red stars in Fig. 4 locate five dwarf spheroidal galaxies that in varying degrees are isolated systems. Two of them, Cetus and And XVIII, are located inside the zero-velocity sphere of the Local Group, and a third, Tucana, lies just outside this surface. Only two dSph galaxies in the volume under consideration are cleanly isolated objects: KKR 25 at a distance of $D_{MW} = 1.93$ Mpc (Karachentsev et al. 2001; Makarov et al. 2012) and KKs 3. One can affirm with virtual certainty that neither of these spheroidal dwarfs have experienced a disturbance from their neighbours over the last ∼ 10 Gyr.

Apart from the two true isolated spheroidal dwarfs in the vicinity of our Local Group, the local volume within $D < 10$ Mpc contains one more known isolated dSph object, Apples I. That galaxy was found accidentally by Pasquali et al. (2005) on an image obtained with ACS HST. The radial velocity of Apples I with respect to the Local Group frame is 661 km s^{-1} and its distance of 8.3 ± 2.2 Mpc is derived from spectroscopic classification of the brightest stars. Since the detection of such objects is difficult, the number of them within 10 Mpc may be considerable.

Recently there have been discussions of two rather deep multi-band surveys over areas of 300 square degrees (Jiang et al. 2014) and 170 square degrees (Hildebrandt & on behalf of the CFHTLenS collaboration 2014). The limiting magnitudes of these surveys could resolve the brightest RGB stars of dSph galaxies if they lie within 4 and 5 Mpc, respectively. Inspection of these images fails to reveal any isolated dSph candidates. Given the relative sky fraction of these surveys (∼ 1 per cent) and their depth, the expected total number of isolated spheroidal dwarfs in the local volume does not exceed $N \sim 900$. However, this quantity corresponds closely with the total number of known galaxies in the local volume. Therefore, the present-day observational data do not reject the presence of a significant population of relic "quenched" dwarfs comparable in number with all other kinds of galaxies. Future deep wide-field surveys of the sky, like Pan-STARRS1 (Tonry et al. 2012), are required to bring clarity to this important aspect of the problem of galaxy formation and evolution.

5 SUMMARY

The key results can be enumerated. (1) The dominance of ancient stars and the lack of any evidence of recent star formation in the CMD justifies the classification of KKs 3 as a dSph. (2) KKs 3 is 2 Mpc from the nearest large galaxy and 1 Mpc from any known dwarf so qualifies as isolated. (3) Although a very old and metal poor population is dominant, this early episode of star formation is probably not enough to explain the breadth of the RGB and the luminosity range of the red clump. (4) KKs 3 sustained limited star formation over many Gyr after its early development but exhausted its star forming fuel in isolation.

ACKNOWLEDGEMENTS

The authors thank Nicolas Martin for constructive comments which helped improve the article. This work is based on observations made with the NASA/ESA Hubble Space Telescope. STScI is operated by the Association of Universities for Research in Astronomy, Inc. under NASA contract NAS 5–26555. The work in Russia is supported by RFBR grants 13–02–90407 and 13–02–92960. We acknowledge the support from RFBR grant 13–02–00780 and Research Program OFN–17 of the Division of Physics, Russian Academy of Sciences.

REFERENCES

Benítez-Llambay A., Navarro J. F., Abadi M. G., Gottlöber S., Yepes G., Hoffman Y., Steinmetz M., 2013, ApJ, 763, L41

Chiboucas K., Karachentsev I. D., Tully R. B., 2009, AJ, 137, 3009

Corwin H. G., de Vaucouleurs A., de Vaucouleurs G., 1985, Southern galaxy catalogue. A catalogue of 5481 galaxies south of declination -17 grad. found on 1.2m UK Schmidt IIIa J plates

Dolphin A. E., 2002, MNRAS, 332, 91

Giovanelli R., Haynes M. P., Adams E. A. K., Cannon J. M., Rhode K. L., Salzer J. J., Skillman E. D., Bernstein-Cooper E. Z., McQuinn K. B. W., 2013, AJ, 146, 15

Girardi L., Bressan A., Bertelli G., Chiosi C., 2000, A&AS, 141, 371

Hildebrandt H., on behalf of the CFHTLenS collaboration, 2014, ArXiv e-prints

Jiang L., Fan X., Bian F., McGreer I. D., Strauss M. A., Annis J., Buck Z., Green R., Hodge J. A., Myers A. D., Rafiee A., Richards G., 2014, ApJS, 213, 12

Karachentsev I. D., Makarov D. I., Kaisina E. I., 2013, AJ, 145, 101

Karachentsev I. D., Makarova L. N., Tully R. B., Wu P.-F., Kniazev A. Y., 2014, MNRAS, 443, 1281

Karachentsev I. D., Sharina M. E., Dolphin A. E., Geisler D., Grebel E. K., Guhathakurta P., Hodge P. W., Karachentseva V. E., Sarajedini A., Seitzer P., 2001, A&A, 379, 407

Karachentseva V. E., Karachentsev I. D., 2000, A&AS, 146, 359

Kirby E. M., Jerjen H., Ryder S. D., Driver S. P., 2008, AJ, 136, 1866

Kopylov A. I., Tikhonov N. A., Fabrika S., Drozdovsky I., Valeev A. F., 2008, MNRAS, 387, L45

Makarov D., Makarova L., Rizzi L., Tully R. B., Dolphin A. E., Sakai S., Shaya E. J., 2006, AJ, 132, 2729

Makarov D., Makarova L., Sharina M., Uklein R., Tikhonov A., Guhathakurta P., Kirby E., Terekhova N., 2012, MNRAS, 425, 709

Makarov D. I., Makarova L. N., 2004, Astrophysics, 47, 229

Makarova L., Koleva M., Makarov D., Prugniel P., 2010, MNRAS, 406, 1152

Martin N. F., Ibata R. A., McConnachie A. W., Mackey A. D., Ferguson A. M. N., Irwin M. J., Lewis G. F., Fardal M. A., 2013, ApJ, 776, 80

Pasquali A., Larsen S., Ferreras I., Gnedin O. Y., Malhotra S., Rhoads J. E., Pirzkal N., Walsh J. R., 2005, AJ, 129, 148

Rizzi L., Tully R. B., Makarov D., Makarova L., Dolphin A. E., Sakai S., Shaya E. J., 2007, ApJ, 661, 815

Salpeter E. E., 1955, ApJ, 121, 161

Schlafly E. F., Finkbeiner D. P., 2011, ApJ, 737, 103

Tonry J. L., Stubbs C. W., Lykke K. R., Doherty P., Shivvers I. S., Burgett W. S., Chambers K. C., Hodapp K. W., Kaiser N., Kudritzki R.-P., Magnier E. A., Morgan J. S., Price P. A., Wainscoat R. J., 2012, ApJ, 750, 99

White S. D. M., Rees M. J., 1978, MNRAS, 183, 341

Whiting A. B., Hau G. K. T., Irwin M., 2002, ApJS, 141, 123

This paper has been typeset from a TEX/ LATEX file prepared by the author.